EUROPEAN ORGANIZATION FOR NUCLEAR RESEARCH

CERN-EP/2002-015
February 13, 2002

Determination of α_s from Hadronic Event Shapes in e^+e^- Annihilation at $192 \leq \sqrt{s} \leq 208$ GeV

The L3 Collaboration

Abstract

Results are presented from a study of the structure of high energy hadronic events recorded by the L3 detector at $\sqrt{s} \geq 192$ GeV. The distributions of several event shape variables are compared to resummed $\mathcal{O}(\alpha_s^2)$ QCD calculations. We determine the strong coupling constant at three average centre-of-mass energies: 194.4, 200.2 and 206.2 GeV. These measurements, combined with previous L3 measurements at lower energies, demonstrate the running of α_s as expected in QCD and yield $\alpha_s(m_Z) = 0.1227 \pm 0.0012 \pm 0.0058$, where the first uncertainty is experimental and the second is theoretical.

Submitted to *Phys. Lett. B*

1 Introduction

The measurement of the energy dependence of the strong coupling constant, α_s, is an important test of Quantum Chromo-Dynamics (QCD). Hadronic events produced in e^+e^- annihilation offer a clean environment to perform such measurements. The high energy phase of the LEP collider gives a unique opportunity to measure QCD observables over a wide energy range and to perform a precise test of the energy dependence of the strong coupling constant. In addition, the study of hadronic events allows to check the validity of the QCD models used for background modelling in other studies, such as new particle searches.

In its last two years, the LEP collider operated at various centre-of-mass energies, $\sqrt{s}$, between 192 and 208 GeV. These are grouped in three samples of average centre-of-mass energies 194.4, 200.2 and 206.2 GeV, corresponding to the ranges $192 \leq \sqrt{s} < 196$ GeV, $200 < \sqrt{s} < 202$ GeV and $\sqrt{s} > 202$ GeV respectively.

We report on measurements of five event shape distributions using 436.8 pb^{-1} of data collected with the L3 detector [1] at these centre-of-mass energies, as detailed in Table 1. To allow a direct comparison with our earlier QCD studies at lower energies [2–6], we follow an identical analysis procedure. The value of α_s is extracted in each energy range by comparing the measured event shape distributions with predictions of second order QCD calculations [7] supplemented by resummed leading and next-to-leading order terms [8–11]. These values are used, together with previous L3 measurements at lower effective centre-of-mass energies, from 30 GeV to 189 GeV, to study the energy evolution of α_s.

2 Event Selection

The criteria for the selection of $e^+e^- \rightarrow q\bar{q} \rightarrow$ *hadrons* events are identical to those used in our previous QCD study at $\sqrt{s} = 189$ GeV [6]. They are based on the measured total visible energy, E_{vis} , the energy imbalances parallel, $E_{\parallel}$, and perpendicular, $E_{\perp}$, to the beam direction and on the cluster multiplicity, N_{cl}. These variables are constructed using energy clusters in the electromagnetic and hadronic calorimeters with a minimum energy of 100 MeV.

The efficiency of the selection criteria and the purity of the data sample are estimated using Monte Carlo events for the process $e^+e^- \rightarrow q\bar{q}(\gamma)$ generated by the KK2F [12] program, interfaced with JETSET PS [13] routines to describe the QCD parton shower evolution and hadronisation. The events are then passed through the L3 detector simulation [14]. The KK2F generator is chosen for its improved simulation of the initial state radiation (ISR) as compared to the PYTHIA [13] model previously used. Background events are simulated with PYTHIA for two-photon events and Z-pair production, KORALZ [15] for the $\tau^+\tau^-(\gamma)$ final state, BHAGENE [16] and BHWIDE [17] for Bhabha events and KORALW [18] for W-pair production.

Hadronic events with hard ISR photons, where the mass of the hadronic system is close to m_Z, are considered as background if the photon energy exceeds $0.18\sqrt{s}$. This important background is reduced to less than 8% of the selected events by applying a cut in the plane of $|E_{\parallel}|/E_{vis}$ *vs.* $E_{vis}/\sqrt{s}$. Additional background arises from W- and Z-pair production. A substantial fraction of these events is removed by a specific selection [5] that forces a 4-jet topology using the Durham algorithm [19], and applies cuts on the cluster multiplicity, $N_{cl} > 40$, the jet resolution parameter, $y^D_{34} > 0.0025$, the energy of the least energetic jet and on the energy fraction carried by the two most energetic jets. The cuts are optimised to maximise the product of efficiency and purity at each energy point. After selection, the W-pair background amounts to 6.4% at $\sqrt{s}$ = 192 GeV and increases to 10.3% at $\sqrt{s}$ = 208 GeV. The Z-pair background is below 0.8%. The selection efficiency, purity and number of selected events for the three energy points are summarised in Table 1.

3 Measurement of Event Shape Variables

The measured global event shape variables are the thrust [20], T, the scaled heavy jet mass [21], ρ, the total, B_T, and wide, B_W, jet broadening variables [9] and the C-parameter [22]. The first four observables are defined in terms of the particle four-momenta, while the C-parameter is derived from the spherocity tensor:

$$\theta^{ij} = \frac{\sum_a p_a^i p_a^j / \mid \vec{p_a} \mid}{\sum_a \mid \vec{p_a} \mid} \quad i,j = 1,2,3\ ,$$

where the sums run over all particles and $\vec{p}_a$ is the momentum vector of the particle a. The C-parameter is defined in terms of the eigenvalues, λ_1, λ_2 and λ_3, of θ^{ij}, as:

$$C = 3(\lambda_1\lambda_2 + \lambda_2\lambda_3 + \lambda_3\lambda_1)\ .$$

For all five variables, improved analytical QCD calculations [8–11] are available. The calculations used here for the jet broadening variables [11] are improved as compared to the previous predictions [9] by a better treatment of quark recoil effects.

After background subtraction, the measured distributions are corrected bin-by-bin for detector effects, acceptance and resolution. The correction factors are the ratios of Monte Carlo distributions at detector level to the distributions at particle level which include all stable charged and neutral particles. [1)] The data are also corrected bin-by-bin for initial and final state photon radiation using Monte Carlo distributions at particle level with and without radiation.

Figures 1 and 2 show the thrust and wide jet broadening distributions corrected to the particle level. The data are compared with the JETSET, HERWIG [23] and ARIADNE [24] QCD models. These models, based on an improved leading-logarithmic approximation parton shower, including QCD coherence effects, are tuned to reproduce the global event shape distributions and the charged particle multiplicity distribution measured at 91.2 GeV [25]. At and above centre-of-mass energies of 200.2 GeV some discrepancies appear for specific values of the observables. Several studies are performed to investigate the reason for such effects. The observed structures in the global event shape distributions are found to depend neither on time nor on detector geomety. The effects of these discrepancies are taken into account in the determination of the systematic uncertainties.

The two main sources of systematic uncertainty in the event shape variable distributions are those on detector correction and background estimation. These uncertainties are estimated by repeating the measurement with different analysis criteria and correction procedures [5, 6]. The uncertainty in the detector correction is estimated with the following tests:

- The effect of different particle fluxes in correcting the measured distribution is estimated by using the HERWIG Monte Carlo program instead of JETSET to simulate the signal. Half of the difference obtained with these two models is taken as a systematic uncertainty.

[1)] All weakly decaying light particles with mean lifetime larger than 3.3×10^{-10} s are considered stable.

- The definition of reconstructed objects used to calculate the observables is changed from calorimetric clusters to a non-linear combination of energies of charged tracks and calorimetric clusters.

- The acceptance is reduced by restricting the analysis to events in the central part of the detector, $|\cos(\theta_T)| < 0.7$, where θ_T is the polar angle of the thrust axis relative to the beam direction. In this region a better energy resolution is found.

Half of the maximum spread between the latter two tests and the original analysis is assigned as a systematic uncertainty.

The uncertainty on the background composition of the selected sample is estimated by repeating the analysis with:

- an alternative criterion to reject the hard initial state photon events based on a cut on the kinematically reconstructed effective centre-of-mass energy ($\sqrt{s'} < 0.92$);

- a variation of the W^+W^- background estimate by applying a full subtraction of the W-pair contribution without preliminary event rejection;

- a variation of the estimated two-photon interaction background by $\pm$ 30%. The Monte Carlo program used to model two-photon interactions is also changed from PYTHIA to PHOJET [26].

For the first two studies, half of the difference between the results of the original analysis and of the systematic check is taken as the systematic uncertainty. In the two-photon case, half of the maximum spread between the new results and the original analysis is considered as a systematic uncertainty. The statistical component of each systematic uncertainty is estimated and removed following the procedure described in reference [6]. The systematic uncertainties obtained from the different sources are then combined in quadrature. For $\sqrt{s} < 196$ GeV, the uncertainties due to the backgrounds are the most important ones. They are $2-3$ times larger than the uncertainties due to detector corrections. For $\sqrt{s} > 200$ GeV, the uncertainty in the detector correction gives the largest systematic contribution, dominated by the effect of reducing the event thrust acceptance in the central part of the detector, but decreases for $<\sqrt{s}> = 206.2$ GeV.

An important test of QCD models is the comparison of the energy evolution of the means of the event shape variables. The mean values of the five variables obtained at $\sqrt{s} > 192$ GeV are given in Table 2. Figure 3 shows the evolution of $< 1 - T >$ and $< B_W >$ as a function of $\sqrt{s}$. Also shown are the energy dependences of these quantities as predicted by JETSET PS, HERWIG, ARIADNE, COJETS [27] and JETSET ME, with an $\mathcal{O}(\alpha_s^2)$ matrix element implementation. For high energies, the JETSET ME and COJETS models are not favoured by the data.

4 Determination of α_s

The QCD predictions for the five event shape observables are based on $\mathcal{O}(\alpha_s^2)$ perturbative QCD calculations with resummed leading and next-to-leading order terms. To compare these calculations at parton level with the experimental distributions, the effects of hadronisation and decays are corrected for with a folding matrix [4] calculated using the JETSET PS Monte Carlo program.

To determine α_s at each energy point, the measured distributions are fitted in the ranges given in Table 3 to the analytical predictions, using the modified-log(R) matching scheme [10] after corrections for hadronisation effects. Figure 4 shows the experimental data together with the result of the QCD fits for the five variables at $< \sqrt{s} > = 206.2$ GeV.

The α_s measurements at the three energy points are summarised in Table 3 together with their experimental and theoretical uncertainties. The former includes the statistical and the experimental systematic uncertainties discussed above. The latter is obtained from estimates [4] of the hadronisation uncertainty and of the uncalculated higher orders in the QCD predictions.

The hadronisation uncertainty is obtained from the variation in the fitted value of α_s due to hadronisation corrections determined by comparing JETSET with HERWIG and ARIADNE models and changing the JETSET fragmentation parameters, b, σ_q and Λ_{LLA} within their errors [25] and turning off Bose-Einstein correlations. The most important variation comes from the change in the fragmentation models and is taken as an estimate of the overall hadronisation uncertainty.

The uncertainty coming from uncalculated higher orders in the QCD predictions is estimated in two independent ways: by varying the renormalisation scale, μ, and by changing the matching scheme. The scale uncertainty is obtained by repeating the fit for different values of the renormalisation scale in the interval $0.5\sqrt{s} \leq \mu \leq 2\sqrt{s}$. The matching scheme uncertainty is obtained from half of the maximum spread given by different algorithms [10]. The largest of these uncertainties is assigned as the theoretical uncertainty due to uncalculated higher orders.

To obtain a combined value for the strong coupling constant, we take the unweighted average of the five α_s values. The overall theoretical uncertainty is obtained from the average hadronisation uncertainty added in quadrature to the average higher order uncertainty. A cross-check of this theoretical uncertainty is obtained from a comparison of α_s measurements from the various event shape variables which are expected to be differently affected by higher order corrections and hadronisation effects. Half of the maximum spread in the five α_s values is found to be consistent with the estimated theoretical uncertainty.

Earlier L3 measurements at $\sqrt{s} = m_Z$ and at reduced centre-of-mass energies determined α_s from four event shape variables only: T, ρ, B_T and B_W, the resummed calculation for the C-parameter not being available. We have determined α_s at these lower energies from the C-parameter and the values are now included in the overall mean α_s and listed in Table 4.

The improved theoretical predictions for the jet broadening variables are used to update our previously published α_s results at effective centre-of-mass energies from 30 GeV up to 189 GeV, as listed in Table 4. The mean α_s values from the five event shape distributions are given in Table 5 together with the experimental and theoretical uncertainties.

Figure 5a compares the energy dependence of the measured α_s values with the prediction from QCD. The theoretical uncertainties are strongly correlated between these measurements. Hence, the energy dependence of α_s is investigated using only experimental uncertainties. The experimental systematic uncertainties on α_s are partially correlated. The background uncertainties are similar for data points in the same energy range but differ between the low energy, Z peak and high energy data sets. The sixteen measurements in Figure 5a are shown with experimental uncertainties only, together with a fit to the QCD evolution equation [28] with $\alpha_s(m_Z)$ as a free parameter, that takes into account the correlation between the various measurements. The covariance matrix for the fit is obtained as follows:

- The statistical uncertainties are taken as uncorrelated.
- The experimental systematic uncertainties are assumed to be uncorrelated between the

three data sets and to have a minimum overlap correlation between different energies within the same data set. This definition consists of assigning to the covariance matrix element the smallest of the two squared uncertainties.

The fit gives a χ^2 of 17.9 for 15 degrees of freedom corresponding to a confidence level of 0.27 yielding a value of α_s:

$$\alpha_s(m_Z) \quad = \quad 0.1227 \ \pm \ 0.0012 \ \pm \ 0.0058 \, .$$

The first uncertainty is experimental and the second theoretical. The latter is obtained from the result of a fit which includes the theoretical uncertainties and their correlations. The covariance matrix is here defined assuming a minimum overlap correlation between energies of the hadronisation as well as the uncalculated higher order uncertainties. The hadronisation uncertainty contribution to the total theoretical uncertainty is ± 0.0026.

A fit with constant α_s gives a χ^2 of 51.7 for 15 degrees of freedom. These measurements support the energy evolution of the strong coupling constant predicted by QCD. The apparent increase of the α_s values obtained at $\sqrt{s} > 194$ GeV compared to the QCD evolution curve is related to the structures seen in the event shape distributions discussed above.

Figure 5b summarises the α_s values determined by L3 from the measurement of the τ branching fractions into leptons [29], Z lineshape [30] and event shape distributions at various energies, together with the QCD prediction obtained from the fit to the event shape measurements only. The band width corresponds to the evolved uncertainty on $\alpha_s(m_Z)$. All the measurements are consistent with the energy evolution of the strong coupling constant predicted by QCD. The uncertainties on these measurements are dominated by the theoretical uncertainty coming from the unknown higher order contributions in the calculations. An improved determination of α_s from these measurements thus awaits improved theoretical calculations of these corrections.

Author List

The L3 Collaboration:

P.Achard,[20] O.Adriani,[17] M.Aguilar-Benitez,[24] J.Alcaraz,[24,18] G.Alemanni,[22] J.Allaby,[18] A.Aloisio,[28] M.G.Alviggi,[28] H.Anderhub,[46] V.P.Andreev,[6,33] F.Anselmo,[9] A.Arefiev,[27] T.Azemoon,[3] T.Aziz,[10,18] P.Bagnaia,[38] A.Bajo,[24] G.Baksay,[16] L.Baksay,[25] S.V.Baldew,[2] S.Banerjee,[10] Sw.Banerjee,[4] A.Barczyk,[46,44] R.Barillère,[18] P.Bartalini,[22] M.Basile,[9] N.Batalova,[43] R.Battiston,[32] A.Bay,[22] F.Becattini,[17] U.Becker,[14] F.Behner,[46] L.Bellucci,[17] R.Berbeco,[3] J.Berdugo,[24] P.Berges,[14] B.Bertucci,[32] B.L.Betev,[46] M.Biasini,[32] M.Biglietti,[28] A.Biland,[46] J.J.Blaising,[4] S.C.Blyth,[34] G.J.Bobbink,[2] A.Böhm,[1] L.Boldizsar,[13] B.Borgia,[38] S.Bottai,[17] D.Bourilkov,[46] M.Bourquin,[20] S.Braccini,[20] J.G.Branson,[40] F.Brochu,[4] J.D.Burger,[14] W.J.Burger,[32] X.D.Cai,[14] M.Capell,[14] G.Cara Romeo,[9] G.Carlino,[28] A.Cartacci,[17] J.Casaus,[24] F.Cavallari,[38] N.Cavallo,[35] C.Cecchi,[32] M.Cerrada,[24] M.Chamizo,[20] Y.H.Chang,[48] M.Chemarin,[23] A.Chen,[48] G.Chen,[7] G.M.Chen,[7] H.F.Chen,[21] H.S.Chen,[7] G.Chiefari,[28] L.Cifarelli,[39] F.Cindolo,[9] I.Clare,[14] R.Clare,[37] G.Coignet,[4] N.Colino,[24] S.Costantini,[38] B.de la Cruz,[24] S.Cucciarelli,[32] J.A.van Dalen,[30] R.de Asmundis,[28] P.Déglon,[20] J.Debreczeni,[13] A.Degré,[4] K.Deiters,[44] D.della Volpe,[28] E.Delmeire,[20] P.Denes,[36] F.DeNotaristefani,[38] A.De Salvo,[46] M.Diemoz,[38] M.Dierckxsens,[2] C.Dionisi,[38] M.Dittmar,[46,18] A.Doria,[28] M.T.Dova,[11,♯] D.Duchesneau,[4] B.Echenard,[20] A.Eline,[18] H.El Mamouni,[23] A.Engler,[34] F.J.Eppling,[14] A.Ewers,[1] P.Extermann,[20] M.A.Falagan,[24] S.Falciano,[38] A.Favara,[31] J.Fay,[23] O.Fedin,[33] M.Felcini,[46] T.Ferguson,[34] H.Fesefeldt,[1] E.Fiandrini,[32] J.H.Field,[20] F.Filthaut,[30] P.H.Fisher,[14] W.Fisher,[36] I.Fisk,[40] G.Forconi,[14] K.Freudenreich,[46] C.Furetta,[26] Yu.Galaktionov,[27,14] S.N.Ganguli,[10] P.Garcia-Abia,[5,18] M.Gataullin,[31] S.Gentile,[38] S.Giagu,[38] Z.F.Gong,[21] G.Grenier,[23] O.Grimm,[46] M.W.Gruenewald,[1] M.Guida,[39] R.van Gulik,[2] V.K.Gupta,[36] A.Gurtu,[10] L.J.Gutay,[43] D.Haas,[5] R.Sh.Hakobyan,[30] D.Hatzifotiadou,[9] T.Hebbeker,[1] A.Hervé,[18] J.Hirschfelder,[34] H.Hofer,[46] M.Hohlmann,[25] G.Holzner,[46] S.R.Hou,[48] Y.Hu,[30] B.N.Jin,[7] L.W.Jones,[3] P.de Jong,[2] I.Josa-Mutuberría,[24] D.Käfer,[1] M.Kaur,[15] M.N.Kienzle-Focacci,[20] J.K.Kim,[42] J.Kirkby,[18] W.Kittel,[30] A.Klimentov,[14,27] A.C.König,[30] M.Kopal,[43] V.Koutsenko,[14,27] M.Kräber,[46] R.W.Kraemer,[34] W.Krenz,[1] A.Krüger,[45] A.Kunin,[14] P.Ladron de Guevara,[24] I.Laktineh,[23] G.Landi,[17] M.Lebeau,[18] A.Lebedev,[14] P.Lebrun,[23] P.Lecomte,[46] P.Lecoq,[18] P.Le Coultre,[46] J.M.Le Goff,[18] R.Leiste,[45] M.Levtchenko,[26] P.Levtchenko,[33] C.Li,[21] S.Likhoded,[45] C.H.Lin,[48] W.T.Lin,[48] F.L.Linde,[2] L.Lista,[28] Z.A.Liu,[7] W.Lohmann,[45] E.Longo,[38] Y.S.Lu,[7] K.Lübelsmeyer,[1] C.Luci,[38] L.Luminari,[38] W.Lustermann,[46] W.G.Ma,[21] L.Malgeri,[20] A.Malinin,[27] C.Maña,[24] D.Mangeol,[30] J.Mans,[36] J.P.Martin,[23] F.Marzano,[38] K.Mazumdar,[10] R.R.McNeil,[6] S.Mele,[18,28] L.Merola,[28] M.Meschini,[17] W.J.Metzger,[30] A.Mihul,[12] H.Milcent,[18] G.Mirabelli,[38] J.Mnich,[1] G.B.Mohanty,[10] G.S.Muanza,[23] A.J.M.Muijs,[2] B.Musicar,[40] M.Musy,[38] S.Nagy,[16] S.Natale,[20] M.Napolitano,[28] F.Nessi-Tedaldi,[46] H.Newman,[31] T.Niessen,[1] A.Nisati,[38] H.Nowak,[45] R.Ofierzynski,[46] G.Organtini,[38] C.Palomares,[18] D.Pandoulas,[1] P.Paolucci,[28] R.Paramatti,[38] G.Passaleva,[17] S.Patricelli,[28] T.Paul,[11] M.Pauluzzi,[32] C.Paus,[14] F.Pauss,[46] M.Pedace,[38] S.Pensotti,[26] D.Perret-Gallix,[4] B.Petersen,[30] D.Piccolo,[28] F.Pierella,[9] M.Pioppi,[32] P.A.Piroué,[36] E.Pistolesi,[26] V.Plyaskin,[27] M.Pohl,[20] V.Pojidaev,[17] J.Pothier,[18] D.O.Prokofiev,[43] D.Prokofiev,[33] J.Quartieri,[39] G.Rahal-Callot,[46] M.A.Rahaman,[10] P.Raics,[16] N.Raja,[10] R.Ramelli,[46] P.G.Rancoita,[26] R.Ranieri,[17] A.Raspereza,[45] P.Razis,[29] D.Ren,[46] M.Rescigno,[38] S.Reucroft,[11] S.Riemann,[45] K.Riles,[3] B.P.Roe,[3] L.Romero,[24] A.Rosca,[8] S.Rosier-Lees,[4] S.Roth,[1] C.Rosenbleck,[1] B.Roux,[30] J.A.Rubio,[18] G.Ruggiero,[17] H.Rykaczewski,[46] A.Sakharov,[46] S.Saremi,[6] S.Sarkar,[38] J.Salicio,[18] E.Sanchez,[24] M.P.Sanders,[30] C.Schäfer,[18] V.Schegelsky,[33] S.Schmidt-Kaerst,[1] D.Schmitz,[1] H.Schopper,[47] D.J.Schotanus,[30] G.Schwering,[1] C.Sciacca,[28] L.Servoli,[32] S.Shevchenko,[31] N.Shivarov,[41] V.Shoutko,[14] E.Shumilov,[27] A.Shvorob,[31] T.Siedenburg,[1] D.Son,[42] P.Spillantini,[17] M.Steuer,[14] D.P.Stickland,[36] B.Stoyanov,[41] A.Straessner,[18] K.Sudhakar,[10] G.Sultanov,[41] L.Z.Sun,[21] S.Sushkov,[8] H.Suter,[46] J.D.Swain,[11] Z.Szillasi,[25,¶] X.W.Tang,[7] P.Tarjan,[16] L.Tauscher,[5] L.Taylor,[11] B.Tellili,[23] D.Teyssier,[23] C.Timmermans,[30] Samuel C.C.Ting,[14] S.M.Ting,[14] S.C.Tonwar,[10,18] J.Tóth,[13] C.Tully,[36] K.L.Tung,[7] J.Ulbricht,[46] E.Valente,[38] R.T.Van de Walle,[30] V.Veszpremi,[25] G.Vesztergombi,[13] I.Vetlitsky,[27] D.Vicinanza,[39] G.Viertel,[46] S.Villa,[37] M.Vivargent,[4] S.Vlachos,[5] I.Vodopianov,[33] H.Vogel,[34] H.Vogt,[45] I.Vorobiev,[34,27] A.A.Vorobyov,[33] M.Wadhwa,[5] W.Wallraff,[1] X.L.Wang,[21] Z.M.Wang,[21] M.Weber,[1] P.Wienemann,[1] H.Wilkens,[30] S.Wynhoff,[36] L.Xia,[31] Z.Z.Xu,[21] J.Yamamoto,[3] B.Z.Yang,[21] C.G.Yang,[7] H.J.Yang,[3] M.Yang,[7] S.C.Yeh,[49] An.Zalite,[33] Yu.Zalite,[33] Z.P.Zhang,[21] J.Zhao,[21] G.Y.Zhu,[7] R.Y.Zhu,[31] H.L.Zhuang,[7] A.Zichichi,[9,18,19] G.Zilizi,[25,¶] B.Zimmermann,[46] M.Zöller.[1]

1 I. Physikalisches Institut, RWTH, D-52056 Aachen, FRG[§]
III. Physikalisches Institut, RWTH, D-52056 Aachen, FRG[§]
2 National Institute for High Energy Physics, NIKHEF, and University of Amsterdam, NL-1009 DB Amsterdam, The Netherlands
3 University of Michigan, Ann Arbor, MI 48109, USA
4 Laboratoire d'Annecy-le-Vieux de Physique des Particules, LAPP,IN2P3-CNRS, BP 110, F-74941 Annecy-le-Vieux CEDEX, France
5 Institute of Physics, University of Basel, CH-4056 Basel, Switzerland
6 Louisiana State University, Baton Rouge, LA 70803, USA
7 Institute of High Energy Physics, IHEP, 100039 Beijing, China[△]
8 Humboldt University, D-10099 Berlin, FRG[§]
9 University of Bologna and INFN-Sezione di Bologna, I-40126 Bologna, Italy
10 Tata Institute of Fundamental Research, Mumbai (Bombay) 400 005, India
11 Northeastern University, Boston, MA 02115, USA
12 Institute of Atomic Physics and University of Bucharest, R-76900 Bucharest, Romania
13 Central Research Institute for Physics of the Hungarian Academy of Sciences, H-1525 Budapest 114, Hungary[‡]
14 Massachusetts Institute of Technology, Cambridge, MA 02139, USA
15 Panjab University, Chandigarh 160 014, India.
16 KLTE-ATOMKI, H-4010 Debrecen, Hungary[¶]
17 INFN Sezione di Firenze and University of Florence, I-50125 Florence, Italy
18 European Laboratory for Particle Physics, CERN, CH-1211 Geneva 23, Switzerland
19 World Laboratory, FBLJA Project, CH-1211 Geneva 23, Switzerland
20 University of Geneva, CH-1211 Geneva 4, Switzerland
21 Chinese University of Science and Technology, USTC, Hefei, Anhui 230 029, China[△]
22 University of Lausanne, CH-1015 Lausanne, Switzerland
23 Institut de Physique Nucléaire de Lyon, IN2P3-CNRS,Université Claude Bernard, F-69622 Villeurbanne, France
24 Centro de Investigaciones Energéticas, Medioambientales y Tecnológicas, CIEMAT, E-28040 Madrid, Spain♭
25 Florida Institute of Technology, Melbourne, FL 32901, USA
26 INFN-Sezione di Milano, I-20133 Milan, Italy
27 Institute of Theoretical and Experimental Physics, ITEP, Moscow, Russia
28 INFN-Sezione di Napoli and University of Naples, I-80125 Naples, Italy
29 Department of Physics, University of Cyprus, Nicosia, Cyprus
30 University of Nijmegen and NIKHEF, NL-6525 ED Nijmegen, The Netherlands
31 California Institute of Technology, Pasadena, CA 91125, USA
32 INFN-Sezione di Perugia and Università Degli Studi di Perugia, I-06100 Perugia, Italy
33 Nuclear Physics Institute, St. Petersburg, Russia
34 Carnegie Mellon University, Pittsburgh, PA 15213, USA
35 INFN-Sezione di Napoli and University of Potenza, I-85100 Potenza, Italy
36 Princeton University, Princeton, NJ 08544, USA
37 University of Californa, Riverside, CA 92521, USA
38 INFN-Sezione di Roma and University of Rome, "La Sapienza", I-00185 Rome, Italy
39 University and INFN, Salerno, I-84100 Salerno, Italy
40 University of California, San Diego, CA 92093, USA
41 Bulgarian Academy of Sciences, Central Lab. of Mechatronics and Instrumentation, BU-1113 Sofia, Bulgaria
42 The Center for High Energy Physics, Kyungpook National University, 702-701 Taegu, Republic of Korea
43 Purdue University, West Lafayette, IN 47907, USA
44 Paul Scherrer Institut, PSI, CH-5232 Villigen, Switzerland
45 DESY, D-15738 Zeuthen, FRG
46 Eidgenössische Technische Hochschule, ETH Zürich, CH-8093 Zürich, Switzerland
47 University of Hamburg, D-22761 Hamburg, FRG
48 National Central University, Chung-Li, Taiwan, China
49 Department of Physics, National Tsing Hua University, Taiwan, China
§ Supported by the German Bundesministerium für Bildung, Wissenschaft, Forschung und Technologie
‡ Supported by the Hungarian OTKA fund under contract numbers T019181, F023259 and T024011.
¶ Also supported by the Hungarian OTKA fund under contract number T026178.
♭ Supported also by the Comisión Interministerial de Ciencia y Tecnología.
♯ Also supported by CONICET and Universidad Nacional de La Plata, CC 67, 1900 La Plata, Argentina.
△ Supported by the National Natural Science Foundation of China.

References

[1] L3 Collaboration, B. Adeva *et al.*, Nucl. Inst. Meth. **A289** (1990) 35;
M. Chemarin *et al.*, Nucl. Inst. Meth. **A349** (1994) 345;
M. Acciarri *et al.*, Nucl. Inst. Meth. **A351** (1994) 300;
G. Basti *et al.*, Nucl. Inst. Meth. **A374** (1996) 293;
A. Adam *et al.*, Nucl. Inst. Meth. **A383** (1996) 342.

[2] L3 Collaboration, O. Adriani *et al.*, Phys. Lett. **B284** (1992) 471;
L3 Collaboration, O. Adriani *et al.*, Phys. Rep. **236** (1993) 1.

[3] L3 Collaboration, M. Acciarri *et al.*, Phys. Lett. **B411** (1997) 339.

[4] L3 Collaboration, M. Acciarri *et al.*, Phys. Lett. **B371** (1996) 137.

[5] L3 Collaboration, M. Acciarri *et al.*, Phys. Lett. **B404** (1997) 390;
L3 Collaboration, M. Acciarri *et al.*, Phys. Lett. **B444** (1998) 569.

[6] L3 Collaboration, M. Acciarri *et al.*, Phys. Lett. **B489** (2000) 65.

[7] Z. Kunszt and P. Nason in "Z Physics at LEP 1", CERN Report 89-08, Vol.I., p. 373.

[8] S. Catani *et al.*, Phys. Lett. **B263** (1991) 491;
S. Catani, G. Turnock and B.R. Webber, Phys. Lett. **B272** (1991) 368;
S. Catani and B.R. Webber, Phys. Lett. **B427** (1998) 377.

[9] S. Catani, G. Turnock and B.R. Webber, Phys. Lett. **B295** (1992) 269.

[10] S. Catani *et al.*, Nucl. Phys. **B407** (1993) 3.

[11] Yu. L. Dokshitzer *et al.*, Journal of High Energy Physics **01** (1998) 11.

[12] KK2F 4.12 Monte Carlo Program:
S. Jadach, B. F. L. Ward and Z. Wąs, Comp. Phys. Comm. **130** (2000) 260.

[13] JETSET 7.4 and PYTHIA 5.7 Monte Carlo Programs:
T. Sjöstrand, CERN-TH-7112/93 (1993), revised august 1995;
T. Sjöstrand, Comp. Phys. Comm. **82** (1994) 74.

[14] The L3 detector simulation is based on GEANT Version 3.15.
See R. Brun *et al.*, "GEANT 3", CERN DD/EE/84-1 (Revised), September 1987.
The GHEISHA program (H. Fesefeldt, RWTH Aachen Report PITHA 85/02 (1985)) is used to simulate hadronic interactions.

[15] KORALZ 4.03 Monte Carlo Program:
S. Jadach, B. F. L. Ward and Z. Wąs, Comp. Phys. Comm. **79** (1994) 503.

[16] BHAGENE3 2.07 Monte Carlo Program:
J. H. Field, Phys. Lett. **B323** (1994) 432;
J. H. Field and T. Riemann, Comp.Phys.Comm. **94** (1996) 53.

[17] BHWIDE 1.01 Monte Carlo Program:
S. Jadach *et al.*, Phys. Lett. **B390** (1997) 298.

[18] KORALW 1.42 Monte Carlo Program:
M. Skrzypek *et al.*, Comp. Phys. Comm. **94** (1996) 216;
M. Skrzypek *et al.*, Phys. Lett. **B372** (1996) 289.

[19] S. Catani *et al.*, Phys. Lett. **B269** (1991) 432;
N. Brown and W.J. Stirling, Z. Phys. **C53** (1992) 629;
S. Bethke *et al.*, Nucl. Phys. **B370** (1992) 310.

[20] S. Brandt *et al.*, Phys. Lett. **12** (1964) 57;
E. Farhi, Phys. Rev. Lett. **39** (1977) 1587.

[21] T. Chandramohan and L. Clavelli, Nucl. Phys. **B184** (1981) 365;
MARK II Collaboration, A. Petersen *et al.*, Phys. Rev. **D37** (1988) 1;
TASSO Collaboration, W. Braunschweig *et al.*, Z. Phys. **C45** (1989) 11.

[22] G. Parisi, Phys. Lett. **B74** (1978) 65;
J. F. Donoghue, F. E. Low, and S. Y. Pi, Phys. Rev. **D20** (1979) 2759.

[23] HERWIG 5.9 Monte Carlo Program:
G. Marchesini and B. Webber, Nucl. Phys. **B310** (1988) 461;
I. G. Knowles, Nucl. Phys. **B310** (1988) 571;
G. Marchesini *et al.*, Comp. Phys. Comm. **67** (1992) 465.

[24] ARIADNE 4.06 Monte Carlo Program:
L. Lönnblad, Comp. Phys. Comm. **71** (1992) 15;
ARIADNE Web page http://shakespeare.thep.lu.se/~ leif/ariadne/.

[25] L3 Collaboration, B. Adeva *et al.*, Z. Phys. **C55** (1992) 39;
S. Banerjee, M. Sc. Thesis, University of Mumbai (1998).

[26] PHOJET 2.01 Monte Carlo Program:
R. Engel, Z. Phys. **C66** (1995) 203;
R. Engel, J. Ranft and S. Roesler, Phys. Rev. **D52** (1995) 1459;
R. Engel and J. Ranft, Phys. Rev. **D54** (1996) 4244.

[27] COJETS 6.23 Monte Carlo Program:
R. Odorico, Comp. Phys. Comm. **72** (1992) 238.

[28] Particle Data Group, D.E. Groom *et al.*, Eur. Phys. J. **C15** (2000) 1.

[29] L3 Collaboration, M. Acciarri *et al.*, Phys. Lett. **B507** (2001) 47.

[30] L3 Collaboration, M. Acciarri *et al.*, Eur. Phys. J. **C16** (2000) 1.

$<\sqrt{s}>$ (GeV)	194.4	200.2	206.2
Integrated Luminosity (pb^{-1})	112.2	117.0	207.6
Selection Efficiency (%)	82.8	85.7	86.0
Sample Purity (%)	81.4	80.6	78.8
Selected Events	2403	2456	4146

Table 1: Summary of integrated luminosity, selection efficiency, sample purity and number of selected hadronic events at the average centre-of-mass energies used in this analysis.

$<\sqrt{s}>$	194.4 GeV	200.2 GeV	206.2 GeV
$<(1-T)>$	$0.0551 \pm 0.0021 \pm 0.0009$	$0.0582 \pm 0.0021 \pm 0.0015$	$0.0569 \pm 0.0017 \pm 0.0016$
$<\rho>$	$0.0439 \pm 0.0014 \pm 0.0007$	$0.0464 \pm 0.0014 \pm 0.0015$	$0.0455 \pm 0.0011 \pm 0.0011$
$<B_T>$	$0.0920 \pm 0.0022 \pm 0.0023$	$0.0950 \pm 0.0021 \pm 0.0025$	$0.0938 \pm 0.0017 \pm 0.0015$
$<B_W>$	$0.0663 \pm 0.0014 \pm 0.0009$	$0.0688 \pm 0.0013 \pm 0.0016$	$0.0682 \pm 0.0011 \pm 0.0009$
$<C>$	$0.2158 \pm 0.0058 \pm 0.0023$	$0.2244 \pm 0.0059 \pm 0.0068$	$0.2195 \pm 0.0049 \pm 0.0035$

Table 2: Mean values of the five event shape variables at different energy points. The first uncertainty is statistical and the second systematic.

	$1-T$	ρ	B_T	B_W	C
Fit Range	0.00−0.25	0.00−0.20	0.02−0.26	0.015−0.210	0.05−0.50
α_s(194.4 GeV)	0.1168	0.1096	0.1152	0.1071	0.1130
Statistical uncertainty	±0.0019	±0.0017	±0.0015	±0.0017	±0.0023
Systematic uncertainty	±0.0015	±0.0014	±0.0015	±0.0013	±0.0024
Overall experimental uncertainty	±0.0024	±0.0022	±0.0021	±0.0021	±0.0033
Overall theoretical uncertainty	±0.0056	±0.0039	±0.0065	±0.0062	±0.0056
χ^2/d.o.f.	2.2 / 9	10.1 / 13	20.2 / 11	9.7 / 12	3.8 / 8
α_s(200.2 GeV)	0.1178	0.1114	0.1164	0.1088	0.1147
Statistical uncertainty	±0.0019	±0.0017	±0.0015	±0.0017	±0.0024
Systematic uncertainty	±0.0027	±0.0028	±0.0018	±0.0014	±0.0016
Overall experimental uncertainty	±0.0033	±0.0033	±0.0023	±0.0022	±0.0029
Overall theoretical uncertainty	±0.0059	±0.0034	±0.0062	±0.0062	±0.0057
χ^2/d.o.f.	7.3 / 9	6.8 / 11	9.6 / 11	10.3 / 12	2.9 / 8
α_s(206.2 GeV)	0.1173	0.1119	0.1163	0.1077	0.1130
Statistical uncertainty	±0.0014	±0.0013	±0.0012	±0.0014	±0.0019
Systematic uncertainty	±0.0016	±0.0014	±0.0017	±0.0013	±0.0021
Overall experimental uncertainty	±0.0021	±0.0019	±0.0021	±0.0019	±0.0028
Overall theoretical uncertainty	±0.0057	±0.0034	±0.0065	±0.0062	±0.0053
χ^2/d.o.f.	7.5 / 9	7.7 / 13	5.9 / 11	7.8 / 12	3.4 / 8

Table 3: Values of α_s measured at $<\sqrt{s}>$ = 194.4, 200.2 and 206.2 GeV from fits of the event shape variables. The fit ranges, the estimated experimental and theoretical uncertainties and the χ^2/d.o.f. of the fit are also given.

$<\sqrt{s}>$	α_s measurement		
(GeV)	from B_T	from B_W	from C
41.4	0.1401±0.0063±0.0119	0.1380±0.0067±0.0091	0.1371±0.0070±0.0102
55.3	0.1321±0.0070±0.0099	0.1191±0.0072±0.0088	0.1197±0.0086±0.0118
65.4	0.1354±0.0067±0.0106	0.1190±0.0062±0.0086	0.1258±0.0039±0.0108
75.7	0.1296±0.0074±0.0097	0.1068±0.0065±0.0084	0.1143±0.0072±0.0094
82.3	0.1270±0.0079±0.0095	0.1083±0.0067±0.0087	0.1153±0.0060±0.0091
85.1	0.1259±0.0069±0.0095	0.1092±0.0080±0.0091	0.1115±0.0045±0.0089
91.2	0.1222±0.0020±0.0080	0.1196±0.0022±0.0052	0.1170±0.0016±0.0076
130.1	0.1178±0.0033±0.0064	0.1089±0.0031±0.0088	0.1151±0.0040±0.0066
136.1	0.1166±0.0035±0.0064	0.1072±0.0041±0.0078	0.1089±0.0047±0.0076
161.3	0.1123±0.0042±0.0067	0.1058±0.0059±0.0068	0.1043±0.0060±0.0057
172.3	0.1105±0.0063±0.0061	0.1062±0.0050±0.0065	0.1121±0.0068±0.0057
182.8	0.1145±0.0022±0.0060	0.1045±0.0021±0.0071	0.1081±0.0029±0.0054
188.6	0.1153±0.0018±0.0067	0.1063±0.0017±0.0078	0.1118±0.0023±0.0055

Table 4: Updated α_s measurements from the jet broadening distributions and the C-parameter measured at $\sqrt{s} < 189$ GeV. The first uncertainty is experimental and the second theoretical.

$<\sqrt{s}>$	α_s measurement from T, ρ, B_T, B_W, C				
(GeV)	α_s	stat	syst	hadr.	hi. order
41.4	0.1418	±0.0053	±0.0030	±0.0055	±0.0085
55.3	0.1260	±0.0047	±0.0056	±0.0066	±0.0062
65.4	0.1331	±0.0032	±0.0042	±0.0059	±0.0064
75.7	0.1204	±0.0024	±0.0059	±0.0060	±0.0053
82.3	0.1184	±0.0028	±0.0053	±0.0060	±0.0051
85.1	0.1152	±0.0037	±0.0051	±0.0060	±0.0055
91.2	0.1210	±0.0008	±0.0017	±0.0040	±0.0052
130.1	0.1138	±0.0033	±0.0021	±0.0031	±0.0046
136.1	0.1121	±0.0039	±0.0019	±0.0038	±0.0045
161.3	0.1051	±0.0048	±0.0026	±0.0026	±0.0044
172.3	0.1099	±0.0052	±0.0026	±0.0024	±0.0048
182.8	0.1096	±0.0022	±0.0010	±0.0023	±0.0044
188.6	0.1122	±0.0014	±0.0012	±0.0022	±0.0045
194.4	0.1123	±0.0018	±0.0016	±0.0020	±0.0047
200.2	0.1138	±0.0018	±0.0021	±0.0020	±0.0046
206.2	0.1132	±0.0014	±0.0016	±0.0019	±0.0047

Table 5: Combined α_s values from the five event shape variables with their uncertainties.

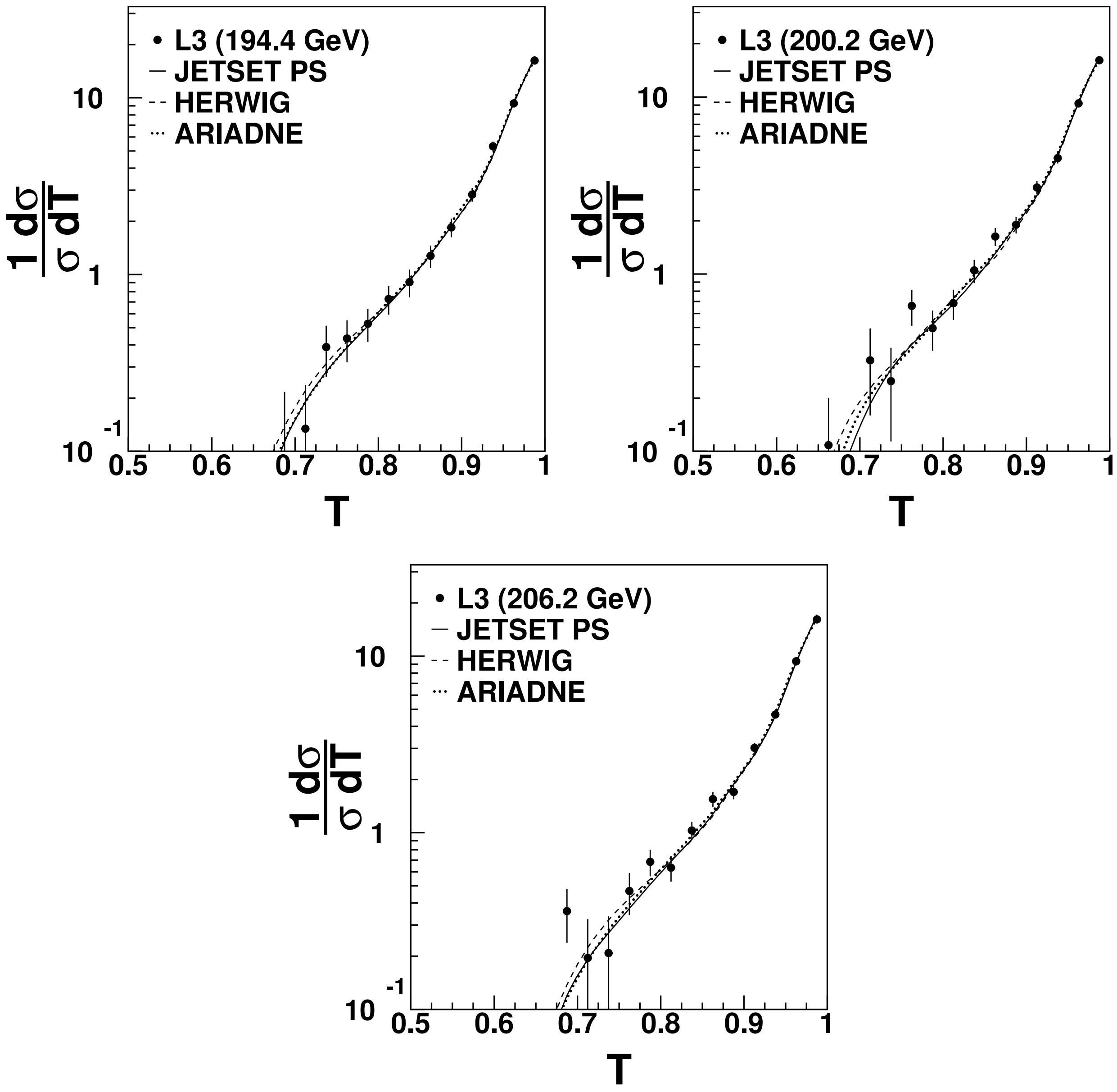

Figure 1: Corrected distributions for the thrust, T, at $<\sqrt{s}>=$ 194.4, 200.2 and 206.2 GeV compared with QCD model predictions. The uncertainties shown are statistical only.

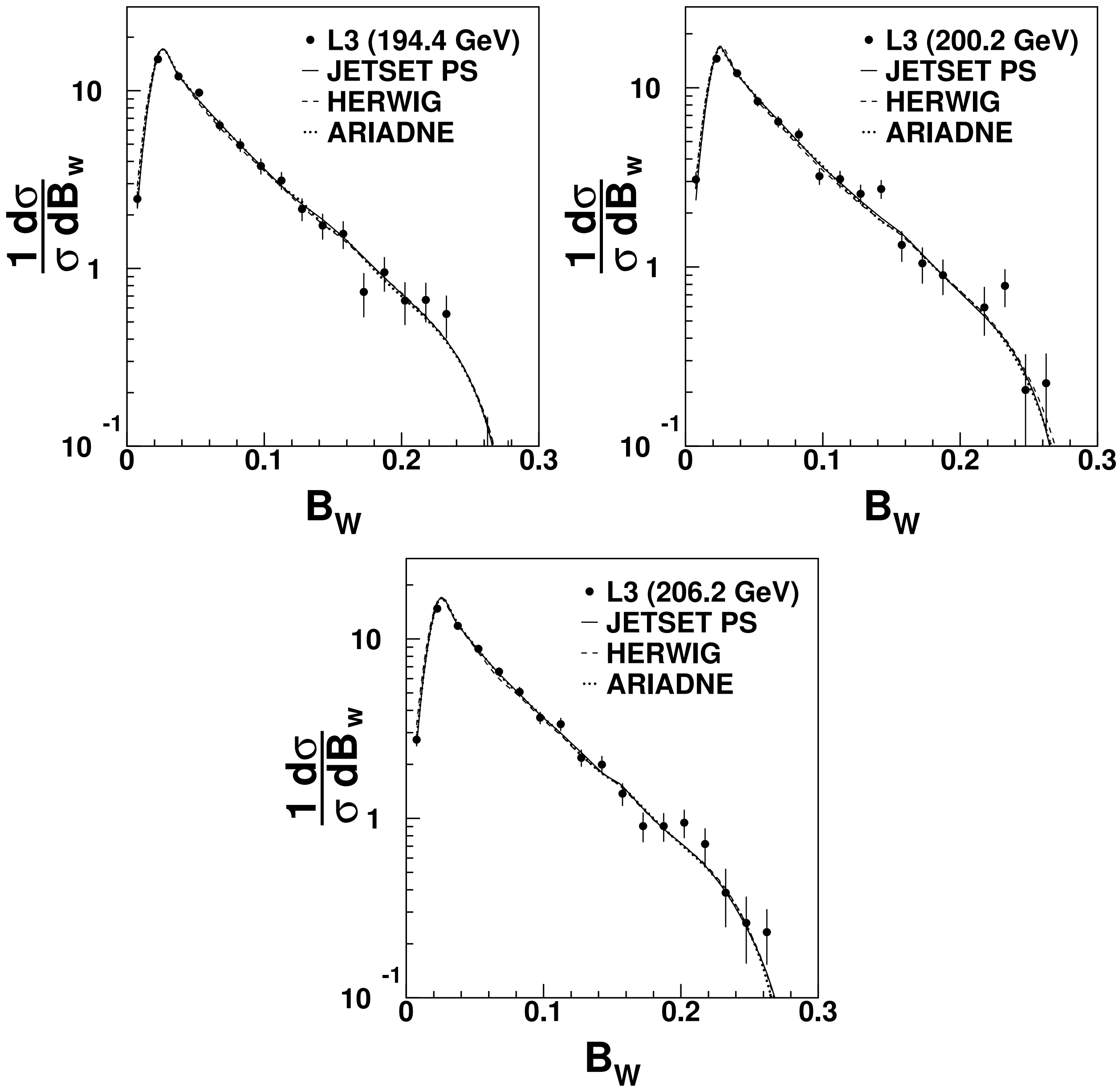

Figure 2: Corrected distributions for the wide jet broadening, B_W, at $<\sqrt{s}>=$ 194.4, 200.2 and 206.2 GeV compared with QCD model predictions. The uncertainties shown are statistical only.

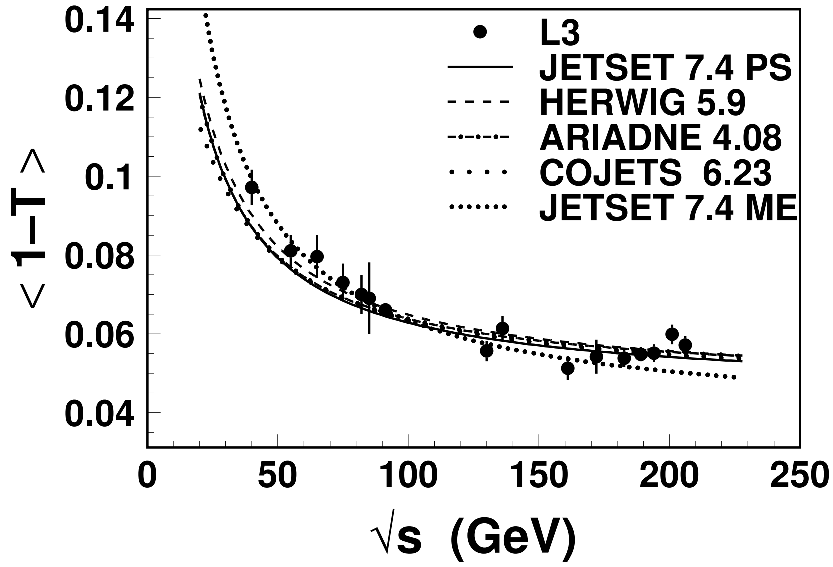

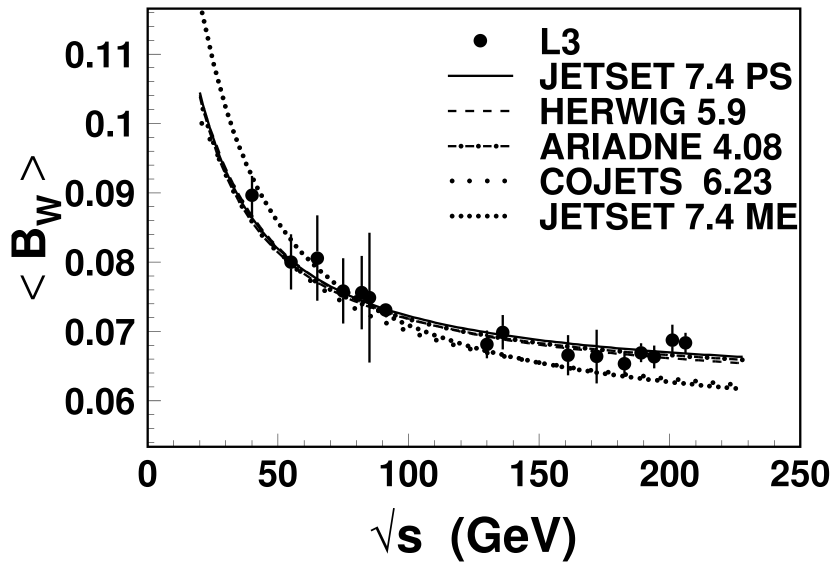

Figure 3: Distribution of a) $< 1 - T >$ and b) $< B_W >$ as a function of the centre-of-mass energy, compared to several QCD models. Lower energy data [2–6] are also presented. The error bars include experimental systematic uncertainties.

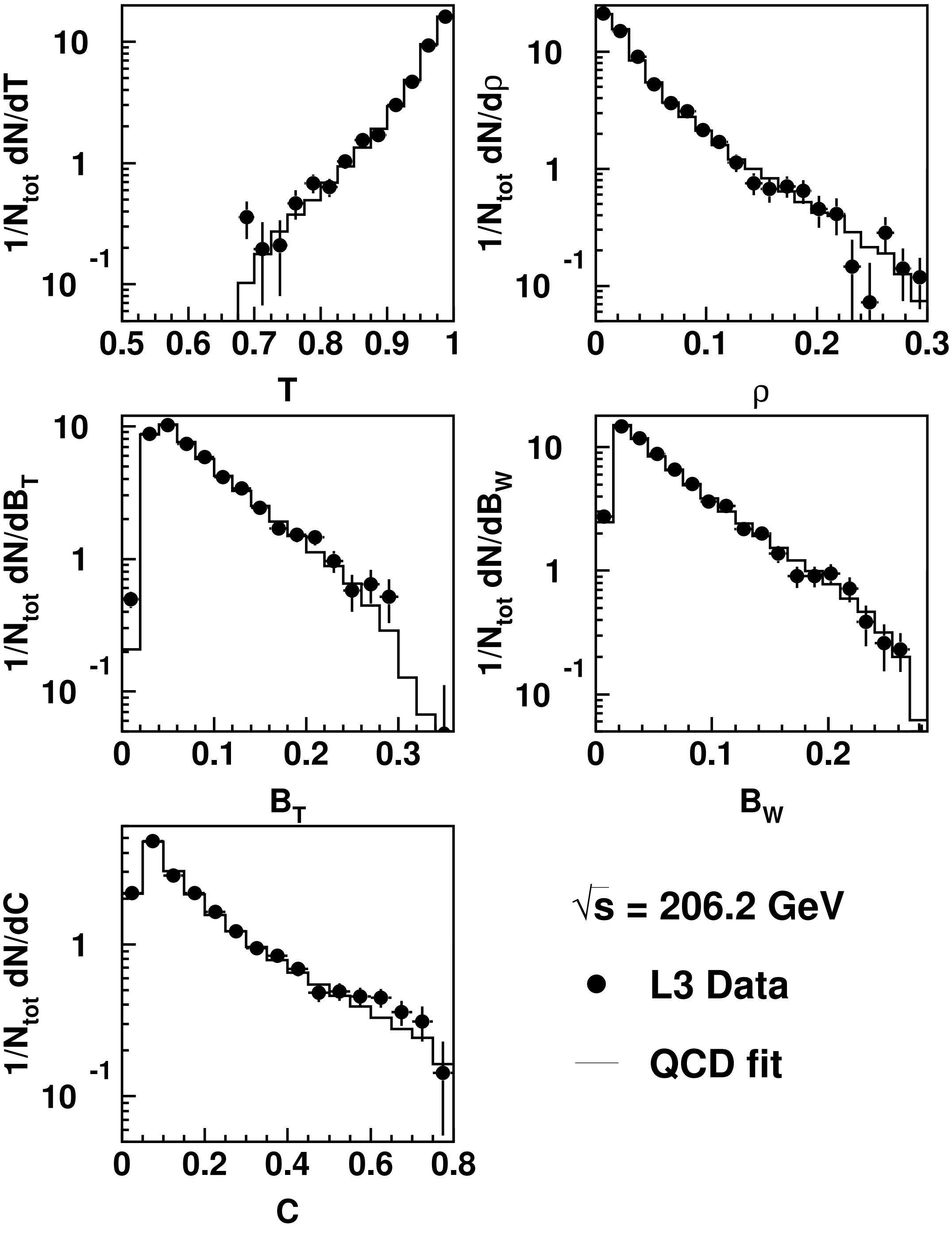

Figure 4: Measured distributions of thrust, T, scaled heavy jet mass, ρ, total, B_T, and wide, B_W, jet broadenings, and C-parameter in comparison with QCD predictions at $<\sqrt{s}>$=206.2 GeV. The error bars include experimental systematic uncertainties.

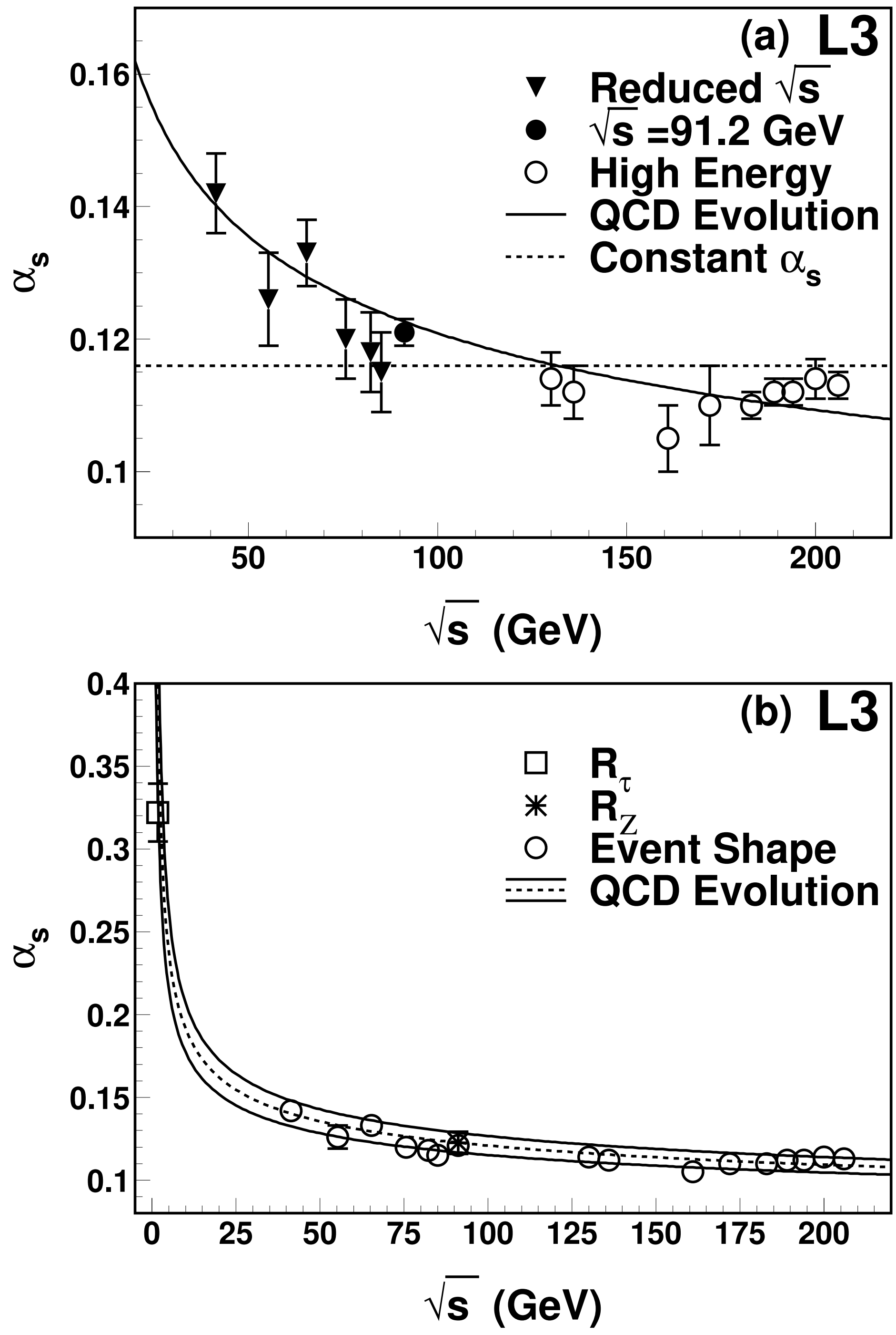

Figure 5: Values of α_{s} determined as a function of $\sqrt{s}$: a) from event shape distributions with experimental uncertainties only. The solid and dashed lines are fits with the energy dependence of α_{s} as expected from QCD and with constant α_{s}, respectively; b) from the measurement of the τ branching fractions into leptons [29], Z lineshape [30] and event shape distributions. The dashed line is a fit to the QCD evolution function to the measurements made from event shape variables. The band width corresponds to the evolved uncertainty on $\alpha_{\mathrm{s}}(m_{\mathrm{Z}})$.